Proceedings of the
47th IEEE Conference on Decision and Control
Cancun, Mexico, Dec. 9-11, 2008

High-Gain Observers in the Presence of Measurement Noise: A Nonlinear Gain Approach

Alexis A. Ball and Hassan K. Khalil
Department of Electrical and Computer Engineering
Michigan State University
East Lansing, Michigan 48824-1226
Email: {ballalex, khalil}@egr.msu.edu

Abstract— **This paper studies a high-gain observer with a nonlinear gain. The nonlinearity is chosen to have a higher observer gain during the transient period and a lower gain afterwards, thus overcoming the tradeoff between fast state reconstruction and measurement noise attenuation. The observer is designed such that the behavior of the innovation process can be controlled separately from the other system states. This is accomplished by assigning one fast eigenvalue, with the remaining eigenvalues chosen relatively slow. Without this key step, the stability analysis for the proposed observer is unattainable. Recently, a switched observer approach has been investigated, but the nonlinear gain approach bypasses the complications associated with switching, with little to no appreciable degradation in performance. This paper presents a new model for the nonlinear observer, accompanied by a discussion focusing on the main ideas behind the proof.**

I. INTRODUCTION

High-gain observers are an important topic in state estimation and feedback control; in the absence of measurement noise, this technique has the ability to simultaneously reject modeling uncertainty and quickly reconstruct the system states [1]. Some of the earlier work performed in the spirt of high-gain observers can be viewed in [2] and [3]; see also [4] and [5] for recent results. The literature on high-gain observers is vast, and the previous papers are in no way inclusive. In order to achieve the objectives of minimizing the effect of measurement noise and fast state estimation, the observer gain (or bandwidth) must be chosen sufficiently high. However, the presence of measurement noise challenges this premise. The effect of measurement noise was studied in [6], [7], and [8], where it was shown that the steady-state estimation error has a component due to modeling uncertainty, which can be attenuated by increasing the gain. Yet, the error has a component due to measurement noise that is amplified by increasing the gain. This tradeoff constrains the observer gain, which reduces the observer's ability to quickly reconstruct the states.

In order to address the aforementioned tradeoff, a switched gain observer was proposed in [7] to force a large gain during the transient period for fast state reconstruction, and allow for a smaller gain once the states were satisfactorily estimated to reduce the effect of noise on the steady-state performance.

This work was supported in part by the National Science Foundation under grant numbers ECS-0400470 and ECCS-0725165.

However, a number of complications are generally associated with a switched system. The time in which the gains are switched, trigger threshold, and system peaking are all issues that must be addressed. Both from an analysis and design/implementation prospective, using a switched observer can be quite tedious. The authors of [9] investigated the use of a deadzone nonlinearity to alternate between two filters of different bandwidths in order to achieve fast state estimation while minimizing the quantization error. The two sets of estimators, similar to [10], were necessary to achieve adequate noise filtering and fast state reconstruction. In [11], the idea of using a deadzone nonlinearity inherent to the structure of the high-gain was proposed and shown to be effective through simulation. Yet, neither [9] or [11] were able to provide a proof for this conjecture due to its inherent challenges. Namely, the form of the nonlinearity to be inserted into the high-gain observer is not an obvious choice. Moreover, even once the appropriate representation was chosen, the nonlinear term present in the observer is manifested in the closed-loop error dynamics in an inconvenient manner; not only is there a nonlinear dependence on the first error state, but the size of the zone plays a role in the size of the ultimate bound. The task of proving that the trajectories starting outside the zone would reach the second phase of the observer gain, and the estimation error would asymptotically approach a small magnitude was difficult, if not impossible, to show before the high-gain observer representation and analysis presented in this work.

An alternative to the switched or nonlinear high-gain observer approach, for the class of problems addressed here, is that of the sliding mode observer. As studied in [12] and [13], the sliding mode observer technique is robust against unknown system inputs, but sensitive to measurement noise. In [14], a bound on the differentiation error was derived for a higher-order sliding mode differentiator. In [8] a direct comparison to the simulation results given in [14] showed that the performance of the sliding mode and high-gain observers in estimating the open-loop derivatives in the presence of measurement noise was comparable. Further information on sliding mode observers can be found in the survey paper [15], and the references therein.

The purpose of this paper is to provide analysis for the nonlinear gain approach. The idea behind the inclusion of

978-1-4244-3124-3/08/$25.00 ©2008 IEEE

a deadzone nonlinearity in the high-gain observer, is to achieve a large gain when the estimation error is outside of the deadzone and the system is still in the transient phase. Hence, the state estimations can approach the true state values significantly fast. When the estimation error is sufficiently small, the error is inside the deadzone and the observer gain is small. Thus, the measurement noise can be attenuated. Section 2 describes the system form and the general setup. Section 3 introduces the observer dynamics and a few of the key points used in the analysis; stated at the end of the section is a theorem concerning the closed-loop system dynamics. A simulation comparing the system performance under the switched, nonlinear, and linear observers is provided in Section 4.

II. PROBLEM FORMULATION AND SYSTEM DESCRIPTION

Consider the nonlinear system

$$\dot{z} = \psi(x, z, \varsigma, u) \quad (1)$$
$$\dot{x} = Ax + B\phi(x, z, \varsigma, u) \quad (2)$$
$$y = Cx + v \quad (3)$$
$$w = \Theta(x, z, \varsigma) \quad (4)$$

where $z \in \mathbb{R}^l$ and $x \in \mathbb{R}^n$ are the system states, $y \in \mathbb{R}$ and $w \in \mathbb{R}^s$ are the measured outputs, $u \in \mathbb{R}$ is the control input, $\varsigma(t) \in \mathbb{R}^p$ represents the exogenous signals, and $v(t) \in \mathbb{R}$ is the measurement noise. Note, that the function $\phi(x, z, \varsigma, u)$ is not necessarily known. Moreover, the model allows for the possibility of zero dynamics. The triple (A, B, C) represents a chain of n integrators. The system defined in (1) - (4) is required to satisfy Assumption 1 below.

Assumption 1:

- $\varsigma(t) \in \mathcal{D} \subset \mathbb{R}^p$, where $\mathcal{D}$ is compact
- $\varsigma(t)$ is continuously differential and both $\varsigma(t)$ and $\dot{\varsigma}(t)$ are bounded
- $v(t)$ is Lebesgue measurable and bounded, where the bound is defined as $|v(t)| \leq \mu$
- ϕ, ψ, and Θ are locally Lipschitz in their arguments, uniformly in ς, over the domain of interest; for each compact subset of (x, z, u) in the domain of interest, the functions satisfy the Lipschitz inequality with a Lipschitz constant independent of ς for all $\varsigma \in \mathcal{D}$

The state feedback controller takes the following form

$$\dot{\theta} = \Gamma(\theta, x, w, \varsigma) \quad (5)$$
$$u = \gamma(\theta, x, w, \varsigma) \quad (6)$$

and meets the requirements listed in Assumption 2.

Assumption 2:

- Γ and γ are locally Lipschitz functions in their arguments, uniformly in ς, over the domain of interest
- Γ and γ are globally bounded functions of x

Let the closed-loop system (1) - (4) under the state feedback controller (5) - (6) be denoted as

$$\dot{\chi} = f_r(\chi, \varsigma) \quad (7)$$

where

$$\chi = \begin{bmatrix} x \\ z \\ \theta \end{bmatrix} \in \mathbb{R}^N,\ f_r(\chi, \varsigma) = \begin{bmatrix} Ax + B\phi(x, z, \varsigma, \gamma) \\ \psi(x, z, \varsigma, \gamma) \\ \Gamma(\theta, x, w, \varsigma) \end{bmatrix}$$

Assumption 3:

- The closed-loop system (7) is uniformly asymptotically stable with respect to a compact positively invariant set $\mathcal{A}$, uniformly in ς
- $\phi(x, z, \varsigma, \gamma)$ is zero in $\mathcal{A}$, uniformly in ς

The high-gain observer is defined as

$$\dot{\hat{x}} = A\hat{x} + B\phi_0(\hat{x}, w, \varsigma, u) + h(y - \hat{x}_1) \quad (8)$$

where

$$h_i(y - \hat{x}_1) = \alpha_i \begin{cases} g_2^i(y - \hat{x}_1), & |y - \hat{x}_1| \leq d \\ g_1^i(y - \hat{x}_1) & \\ \quad - (g_1^i - g_2^i)d\,\mathrm{sign}(y - \hat{x}_1), & |y - \hat{x}_1| > d \end{cases}$$

The variable d is the size of the deadzone nonlinearity, which is defined as $[-d, d]$. The observer gains are defined as

$$g_1 = 1/\varepsilon_1 \text{ and } g_2 = 1/\varepsilon_2, \text{ where } \varepsilon_1 < \varepsilon_2$$

Both ε_1 and ε_2 are small positive parameters. The α_i's are designed such that the roots of

$$s^n + \alpha_1 s^{n-1} + \cdots + \alpha_{n-1} s + \alpha_n = 0 \quad (9)$$

have negative real parts. The function ϕ_0 is chosen to be a nominal model of ϕ.

Assumption 4:

- ϕ_0 is locally Lipschitz in its arguments, uniformly in ς, over the domain of interest
- ϕ_0 is globally bounded in x and zero in $\mathcal{A}$

The output feedback controller is obtained by replacing x in (5) - (6) with $\hat{x}$.

III. OBSERVER DYNAMICS

For the closed-loop system analysis, the observer dynamics are replaced by the equivalent dynamics of the scaled estimation error found in [6]:

$$\tilde{\eta} = D(\varepsilon_1)[x - \hat{x}] \quad (10)$$

where $D(\varepsilon_1) = \mathrm{diag}[1, \varepsilon_1, \cdots, \varepsilon_1^{n-1}]$. The closed-loop system under the output feedback controller can be written as

$$\dot{\chi} = f(\chi, \varsigma, D^{-1}(\varepsilon_1)\tilde{\eta}) = \begin{bmatrix} Ax + B\phi(x, z, \varsigma, \gamma(\theta, x - D^{-1}(\varepsilon_1)\tilde{\eta}, w, \varepsilon)) \\ \psi(x, z, \varsigma, \gamma(\theta, x - D^{-1}(\varepsilon_1)\tilde{\eta}, w, \varepsilon)) \\ \Gamma(\theta, x - D^{-1}(\varepsilon_1)\tilde{\eta}, w, \varepsilon) \end{bmatrix} \quad (11)$$

$$\varepsilon_1\dot{\tilde{\eta}} = A_0\tilde{\eta} + \varepsilon_1^n B\delta(\chi, \varsigma, w, D^{-1}(\varepsilon_1)\tilde{\eta}) - B_0\psi - \frac{\varepsilon_1}{\varepsilon_2}Q_0\xi \quad (12)$$

where

$$A_0 = \begin{bmatrix} -\alpha_1 & 1 & \cdots & \cdots & 0 \\ -\alpha_2 & 0 & 1 & \cdots & 0 \\ \vdots & & & \ddots & \vdots \\ -\alpha_{n-1} & \cdots & \cdots & 0 & 1 \\ -\alpha_n & \cdots & \cdots & \cdots & 0 \end{bmatrix}, B_0 = \begin{bmatrix} -\alpha_1 \\ -\alpha_2 \\ \vdots \\ -\alpha_{n-1} \\ -\alpha_n \end{bmatrix}$$

$$\psi = \begin{cases} \tilde{\eta}_1, & |\tilde{\eta}_1 + v| \leq d \\ -v + d\ \text{sign}(\tilde{\eta}_1 + v), & |\tilde{\eta}_1 + v| > d \end{cases}$$

and

$$\xi_i = (\frac{\varepsilon_1}{\varepsilon_2})^{i-1}(v + \psi),\ Q_0 = \text{diag}[\alpha_1, \alpha_2, \ldots, \alpha_n]$$

The function $\delta(\chi, \varsigma, w, D^{-1}(\varepsilon_1)\tilde{\eta})$ is defined as $\phi(x, z, \varsigma, \gamma(\theta, \hat{x}, w, \varsigma)) - \phi_0(\hat{x}, w, \varsigma, \gamma(\theta, \hat{x}, w, \varsigma))$, and the matrix A_0 is Hurwitz. Note, that except for the presence of negative powers of ε_1 in the $D^{-1}(\varepsilon_1)\tilde{\eta}$ term, (11) - (12) appear in the standard singularly perturbed form [16]. Consider the additional scaling for the observer dynamics as

$$\eta = D(\varepsilon_2)[x - \hat{x}] \tag{13}$$

where (13) is utilized only once the error $y - \hat{x}_1$ settles in the zone $[-d, d]$. Hence, the observer dynamics for η, after entering the zone, are denoted as

$$\varepsilon_2 \dot{\eta} = A_0\eta + \varepsilon_2^n B\delta(\chi, \varsigma, w, D^{-1}(\varepsilon_2)\eta) + B_0 v \tag{14}$$

A key difference in the observer dynamics of (12) and (14), is that (12) has a nonlinear dependence on $\tilde{\eta}_1$ that does not appear in (14). In both representations, δ is a globally bounded function in $\hat{x}$, implying that it is also globally bounded in $D^{-1}(\varepsilon_1)\tilde{\eta}$ and $D^{-1}(\varepsilon_2)\eta$ for (12) and (14), respectively. Thus, there is a constant $L_\delta > 0$, independent of ε_1 and ε_2, such that $\|\delta\| \leq L_\delta$ for all $\chi \in \Omega_c$ and $\tilde{\eta}$, $\eta \in \mathbb{R}^n$; $\Omega_c \subset \mathcal{R}$ and is bounded, where $\mathcal{R}$ is an open connected subset of the region of attraction (which contains $\mathcal{A}$). Moreover, given the functions f and δ are globally bounded in $D^{-1}(\varepsilon_1)\tilde{\eta}$, the behavior of the closed-loop system under output feedback (11) - (12) can be linked to that of standard singularly perturbed systems. The slow dynamics of (11) can be approximated by $\varepsilon_1 = 0$, which yields $\tilde{\eta} = 0$. This reduces (11) to the closed-loop system (7) under the state feedback controller (5) - (6).

Consider the representation of the fast equation (12) for $\chi \in \Omega_c$. Given A_0 is Hurwitz, the solution matrix S to the Lyapunov equation $SA_0 + A_0^T S = -I$ is symmetric and positive definite. Let the Lyapunov function candidate for (12) be chosen as $W = \tilde{\eta}^T S\tilde{\eta}$. It can be shown that

$$\dot{W} \leq -\frac{1}{2\varepsilon_1}\|\tilde{\eta}\|^2,\ \forall \|\tilde{\eta}\| \geq r_1 \tag{15}$$

for $r_1 = \varepsilon_1^n\sigma_1 + (\mu + d)\sigma_2 + \frac{\varepsilon_1}{\varepsilon_2}(2\mu + d)\sigma_3$ and σ_1, σ_2, $\sigma_3 > 0$. To ensure that the trajectories remain inside some set, regardless the scaling used in the error dynamics, take the above Lyapunov candidate function for $\tilde{\eta}$, and apply the following transformation

$$\tilde{\eta} = D\left(\frac{\varepsilon_1}{\varepsilon_2}\right)\eta \tag{16}$$

where $D(\frac{\varepsilon_1}{\varepsilon_2}) = D(\varepsilon_1)D^{-1}(\varepsilon_2)$ which leads to $W = \eta^T D(\frac{\varepsilon_1}{\varepsilon_2})SD(\frac{\varepsilon_1}{\varepsilon_2})\eta$. For trajectories inside the zone, using (14), it can be shown that

$$\dot{W} \leq -\frac{1}{2\varepsilon_2}\|\eta\|^2,\ \forall \|\eta\| \geq r_2 \tag{17}$$

for $r_2 = \varepsilon_2^n\sigma_1 + \mu\sigma_2$ and where the fact that $\|D\| \leq 1$ is utilized. Choose $c_1 > \lambda_{max}(S)r_1^2$ and $c_2 > \lambda_{max}(DSD)r_2^2$. Then, take $c_3 > \max\{c_1, c_2\}$ such that the initial conditions are contained in the set

$$\{W \leq c_3\} \tag{18}$$

Then,

$$\dot{W} \leq -\frac{1}{2\varepsilon_2\|S\|}W,\ \forall\ W \geq c_3 \tag{19}$$

which shows that (18) is a positively invariant set. Moreover, it will be shown that all trajectories starting in (18) will reach the positively invariant set

$$\Sigma = \{W \leq (\varepsilon_2^n\sigma_4 + \mu\sigma_5)^2\} \cap \{|\eta_1| \leq L\mu\} \tag{20}$$

where the first component results from (17). The second component intersecting the first set is described as a positively invariant strip of the following form

$$\{|x_1 - \hat{x}_1| \leq L\mu\} \tag{21}$$

where $L > \frac{1}{\theta}$ and $0 < \theta < 1$. The zone size d is chosen as $d > (L + 1)\mu$ to ensure that (21) implies that

$$|x_1 - \hat{x}_1 + v| \leq d \tag{22}$$

Furthermore, the choice of d may have an affect on the closed-loop system dynamics; if d is chosen too large, the dynamics of the observer may be too slow for the separation principle to apply. This would result in χ growing unbounded before the fast variables enter a positively invariant set. Thus, d should be chosen as small as possible, while still meeting the above requirements. It is required that the trajectories will reach the strip (21) in finite time and stay in thereafter.

When the trajectories are outside the strip (21), it is crucial that they move towards the strip, reaching it in finite time. Once inside the strip, the trajectories should be confined to that strip for all time. This is accomplished by designing A_0 with one fast eigenvalue along with $n - 1$ slow eigenvalues. In this case, (9) is written as

$$(s^{n-1} + \beta_1 s^{n-2} + \cdots + \beta_{n-2}s + \beta_{n-1})(s + \kappa) = 0$$

where the first polynomial is Hurwitz with $\mathcal{O}(1)$ roots and $\kappa \gg 1$. Thus, the fast component is associated with the pole at $-\kappa$. To represent the estimation error in the singularly perturbed form, A_0, B_0, and Q_0 are represented as $A_0 = A_{01}\kappa + A_{02}$, $B_0 = B_{01}\kappa + B_{02}$, and $Q_0 = Q_{01}\kappa + Q_{02}$. As in [6], the procedure from [16] is used to transform the

system (14) into the standard singularly perturbed form via the change of coordinates

$$\begin{bmatrix} \tilde{\zeta} \\ \tilde{\eta}_1 \end{bmatrix} = T\tilde{\eta} \tag{23}$$

where

$$T = \begin{bmatrix} Y \\ Z \end{bmatrix} \text{ and } T^{-1} = \begin{bmatrix} M & N \end{bmatrix}$$

with $M \in \mathbb{R}^{n\times(n-1)}$ and $Y \in \mathbb{R}^{(n-1)\times n}$. It can be shown that the observer dynamics for $\tilde{\eta}$, used for the analysis outside the strip, take the following representation

$$\begin{aligned} \varepsilon_1\dot{\tilde{\zeta}} &= YA_{02}M\tilde{\zeta} + \varepsilon_1^n YB\delta - YB_{02}\psi \\ &\quad - \frac{\varepsilon_1}{\varepsilon_2}Y(Q_{01}\kappa + Q_{02})\xi \end{aligned} \tag{24}$$

$$\begin{aligned} \varepsilon_1\dot{\tilde{\eta}}_1 &= -\kappa\tilde{\eta}_1 + \tilde{\zeta}_1 + (\beta_1+\kappa)\psi \\ &\quad - \frac{\varepsilon_1}{\varepsilon_2}(\beta_1+\kappa)(v+\psi) \end{aligned} \tag{25}$$

where $YA_{02}M$ is by design a Hurwitz matrix. The coefficient of ξ in (24) is $\mathcal{O}(\kappa\frac{\varepsilon_1}{\varepsilon_2})$; thus, $\kappa\frac{\varepsilon_1}{\varepsilon_2}$ needs to be chosen as $\mathcal{O}(1)$ in order to place the system in singularly perturbed form.

The observer dynamics for η in the singularly perturbed form are

$$\varepsilon_2\dot{\zeta} = YA_{02}M\zeta + \varepsilon_2^n YB\delta + YB_{02}v \tag{26}$$

$$\varepsilon_2\dot{\eta}_1 = \zeta_1 - \kappa\eta_1 - (\beta_1+\kappa)v \tag{27}$$

and are only utilized for the analysis inside the strip (21).

The fact that the strip (21) is positively invariant can be shown by calculating the derivative of $W_2 = \frac{1}{2}\eta_1^2$ along the trajectories of (26) - (27), leading to

$$\dot{W}_2 \le -\frac{2(1-\theta)\kappa}{\varepsilon_2}W_2, \ \forall W_2 \ge \frac{1}{2}L^2\mu^2 \tag{28}$$

To show that the trajectories reach the strip (21) in finite time, the derivative of $W_2 = \frac{1}{2}\tilde{\eta}_1^2$ (note that $\tilde{\eta}_1 = \eta_1$) is calculated along the trajectories of (24) - (25). It can be shown that

$$\begin{aligned} \dot{W}_2 &\le -\frac{(1-\theta)(\kappa+\beta_1)}{\varepsilon_2}\tilde{\eta}_1^2, \\ &\qquad \forall|\tilde{\eta}_1| \ge \mu\frac{(\kappa+\beta_1) + \frac{\varepsilon_2}{\varepsilon_1}L_{\tilde{\zeta}_1}}{\theta(\kappa+\beta_1) - \frac{\varepsilon_2}{\varepsilon_1}\beta_1} \end{aligned} \tag{29}$$

for $|\tilde{\eta}_1 + v| \le d$ and

$$\begin{aligned} \dot{W}_2 &\le -\frac{(1-\theta)\kappa}{\varepsilon_2}\tilde{\eta}_1^2, \\ &\quad \forall|\tilde{\eta}_1| \ge \frac{\mu}{\theta} + \frac{\varepsilon_2}{\theta\kappa}\left(\frac{L_{\tilde{\zeta}_1}}{\varepsilon_1} + \beta_1\left[\frac{\mu}{\varepsilon_1} + d(\frac{1}{\varepsilon_1} - \frac{1}{\varepsilon_2})\right]\right) \end{aligned} \tag{30}$$

for $|\tilde{\eta}_1 + v| > d$, where in the latter case the fact that $\tilde{\eta}_1[\tilde{\eta}_1 + v - d\text{sign}(\tilde{\eta}_1 + v)] > 0$ is used, which follows from $|v| < d$. Note that $L_{\tilde{\zeta}_1} > 0$. The lower bounds on $|\tilde{\eta}_1|$ in (29) and (30) can be made arbitrarily close to $\frac{\mu}{\theta}$ by choosing κ large enough. By choosing $L\mu > \frac{\mu}{\theta}$, $\dot{W}_2 \le -\frac{2(1-\theta)\kappa}{\varepsilon_2}W_2$, $\forall|\tilde{\eta}_1| \ge L\mu$.

If $\eta_1(t_0)$ is outside the strip (21), it can be seen from (28) that

$$W_2(\eta_1(t)) \le W_2(\eta_1(t_0))\exp\left(-\frac{2(1-\theta)}{\varepsilon_2}\kappa(t-t_0)\right) \tag{31}$$

Therefore, η_1 will reach the strip (21) within the time interval $[t_0, t_0 + T_s(\varepsilon_2)]$, where

$$T_s(\varepsilon_2) = \frac{\varepsilon_2}{(1-\theta)\kappa}\ln\left(\frac{L_{W_2}}{\sqrt{1/2}L\mu}\right) \tag{32}$$

Referring back to (17), it is clear that if $\eta(t_0)$ is outside of Σ, then

$$W(\eta(t)) \le W(\eta(t_0))\exp\left(-\frac{1}{2\varepsilon_2\|S\|}(t-t_0)\right) \tag{33}$$

which shows that η reaches the set $W \le (\varepsilon_2^n\sigma_4 + \mu\sigma_5)^2$ within the time interval $[t_0, t_0 + T_u(\varepsilon_2)]$, where

$$T_u(\varepsilon_2) = 4\varepsilon_2\|S\|\ln\left(\frac{L_W}{\varepsilon_2^n\sigma_4}\right) \to 0 \text{ as } \varepsilon_2 \to 0 \tag{34}$$

Therefore, it follows from (32) and (34) that $\tilde{\eta}$ will reach the set Σ within the time interval $[t_0, t_0 + T(\varepsilon_2)]$, where

$$T(\varepsilon_2) = T_u(\varepsilon_2) + T_s(\varepsilon_2) \tag{35}$$

The remaining argument for the boundness of all trajectories, ultimate boundness where the trajectories come close to the set $\mathcal{A}\times\{x - \hat{x} = 0\}$, and closeness of trajectories concerns the slow variables, and will not be included here. A similar approach for the slow variables can be found in [11]. One additional important point not included in the work of [11], but relevant here, is that ε_2 is an upper bound on ε_1. Therefore, as $\varepsilon_2 \to 0$ so does ε_1. The above discussion can now be summarized with a theorem.

Theorem 1 *Let Assumption 1 through 4 hold. Moreover, let $\mathcal{M}$ be any compact set in the interior of $\mathcal{R}$ and $\mathcal{N}$ be any compact subset of $\mathbb{R}^n$, where $\chi(t_0) \in \mathcal{M}$ and $\hat{x}(t_0) \in \mathcal{N}$.*

- *There exist constants $c_a > 0$ and $\mu^* > 0$ such that for each $\mu < \mu^*$ there is a constant $\varepsilon_a = \varepsilon_a(\mu) > c_a\mu^{\frac{1}{n}}$, with $\lim_{\mu\to 0}\varepsilon_a(\mu) = \varepsilon_a^* > 0$, such that for each $\varepsilon_2 \in (c_a\mu^{\frac{1}{n}}, \varepsilon_a]$ the trajectories of the closed-loop system are bounded for all $t \ge 0$;*

- *There exist $\mu_1^* > 0$ and a class $\mathcal{K}$ function ρ_1 such that for every $\mu < \mu_1^*$ and every $\Upsilon_1 > \rho_1(\mu)$, there are constants $T_1 = T_1(\Upsilon_1) \ge 0$ and $\varepsilon_b = \varepsilon_b(\mu, \Upsilon_1) > c_a\mu^{\frac{1}{n}}$, with $\lim_{\mu\to 0}\varepsilon_b(\mu, \Upsilon_1) = \varepsilon_b^*(\Upsilon_1) > 0$, such that for each $\varepsilon_2 \in (c_a\mu^{\frac{1}{n}}, \varepsilon_b]$*

$$\max\{|\chi(t)|_{\mathcal{A}}, \|x(t) - \hat{x}(t)\|\} \le \Upsilon_1, \ \forall t \ge T_1 \tag{36}$$

- *There exist $\mu_2^* > 0$ and a class $\mathcal{K}$ function ρ_2 such that for every $\mu < \mu_2^*$ and every $\Upsilon_2 > \rho_2(\mu)$, there is a constant $\varepsilon_c = \varepsilon_c(\mu, \Upsilon_2) > c_a\mu^{\frac{1}{n}}$, with $\lim_{\mu\to 0}\varepsilon_c(\mu, \Upsilon_2) = \varepsilon_c^*(\Upsilon_2) > 0$, such that for each $\varepsilon_2 \in (c_a\mu^{\frac{1}{n}}, \varepsilon_c]$*

$$\|\chi(t) - \chi_r(t)\| \le \Upsilon_2, \ \forall t \ge t_0 \tag{37}$$

where $\chi_r(t)$ is the solution of (7) with $\chi_r(t_0) = \chi(t_0)$.

The complete proof of Theorem 1 will appear elsewhere.

IV. SIMULATION

The purpose of this section is to provide a performance comparison between the linear, switched, and nonlinear high-gain observers. The system under consideration is a field controlled DC motor [17], where it is desired that the shaft angular position track a reference signal as shown in Fig. 1. The system is represented as

$$\dot{x}_1 = x_2 \tag{38}$$
$$\dot{x}_2 = \phi(x, z, u) \tag{39}$$
$$\dot{z} = \psi(x, z, u) \tag{40}$$
$$y = x_1 + v \tag{41}$$
$$w = z \tag{42}$$

where x_1 is the rotor position, x_2 the rotor angular velocity, and z the armature current.

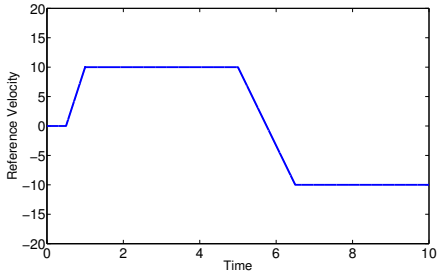

Fig. 1. Velocity reference trajectory ($\dot{r}$)

The design of the controller to achieve tracking is based on feedback linearization. The field current is used as the source of control and is denoted by u. The controller expression is $u = \frac{10}{w}(0.11\hat{x}_2 + \ddot{r} - 100(y - r) - 20(\hat{x}_2 - \dot{r}))$, where standard feedback linearization techniques were applied. The functions above are defined as $\phi(x, z, u) = -0.1x_2 + 0.1zu$ and $\psi(x, z, u) = -2z - 0.2x_2u + 200$. The estimate $\hat{x}_2$ is saturated outside [-20, 20]. The nominal value for ϕ used in the observer is $\phi_0(\hat{x}, w, u) = -0.11x_2 + 0.1wu$. The observer is second-order, given that the state z is measurable and need not be estimated. The remaining observer parameters are chosen as $\alpha_1 = 71$, $\alpha_2 = 70$, $\varepsilon_1 = 0.0005$, and $\varepsilon_2 = 0.01$. The initial conditions are set at $x_1(0) = x_2(0) = \hat{x}_2(0) = 0$, $\hat{x}_1(0) = \pi$, and $z(0) = 100$ to match values consistent with the physical system. It is also important to note that $x_1(0)$ and $\hat{x}_1(0)$ are deliberately chosen to be unequal to ensure some sort of transient response in the system. The measurement noise v is generated using the Simulink block "Uniform Random Noise", where the magnitude is limited to [-0.0016, 0.0016] and the sampling time is set at 0.0008 seconds. The noise magnitude choice is based on a 1000 c/r encoder. The value of d for both the switched observer threshold and the deadzone in the nonlinear observer is 0.005. In the switched observer, it was shown in [6] that if the system switches before the transient response of the estimates of the higher order derivatives has subsided, the value of $y - \hat{x}_1$ could leave the valid switching threshold. If this occurs, the system could be susceptible to multiple switching until all of the trajectories recover from peaking. Thus, the switched observer requires the additional component of a switching timer, based on the peaking period, that prevents the observer from switching before the trajectories of the estimation error have reached a positively invariant set. The delay timer is set for 0.15 seconds; details on how to choose this value can be found in [6].

Fig. 2 shows the transient response of the error $x_2 - \hat{x}_2$ for the observers. As expected, the switched observer captures the behavior of the linear observer with the parameter ε_1. Unlike the switched observer, the nonlinear observer does not wait for the transients to subside in both states before entering the zone and subsequently changing the value of the parameter ε. Thus, the nonlinear observer does not exactly mimic the transient response of the linear observer shown in Fig. 2(c). However, the nonlinear observer does achieve faster state reconstruction than the linear observer with ε_2.

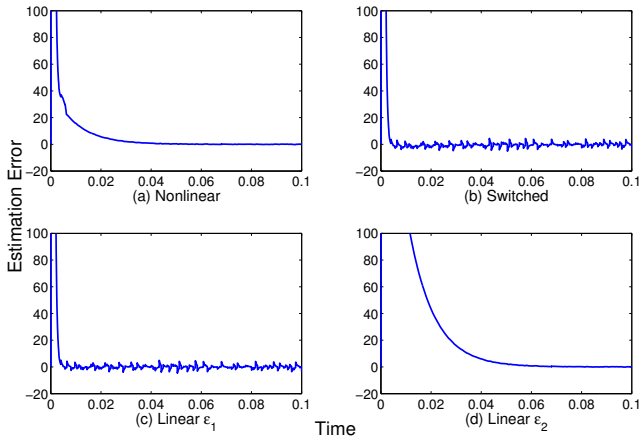

Fig. 2. Transient response for the error $x_2 - \hat{x}_2$ vs. time

In Fig. 3, the steady-state behavior of the nonlinear, switched, and linear (with the parameter ε_2) observers is identical. The linear observer, in Fig. 3(c), with the larger gain is unable to sufficiently attenuate the measurement noise. This is expected, given the smaller value of ε (larger gain) is likely to amplify the noise. In the case of the steady-state response, the nonlinear and switched high-gain observers attenuate the measurement noise in an identical manner.

Fig. 4 shows the tracking error $x_2 - \dot{r}$ during the transient response resulting from the nonlinear, switched, and linear high-gain observer schemes. Given the switched observer waits for all system transients to dissipate before changing the gain, the transient response of the nonlinear observer is slightly slower. However, the steady-state response for the nonlinear, switched, and linear (with ε_2) high-gain observers is identical, as shown in Fig. 5. Thus, the nonlinear observer is able to bypass the complexity associated with the switched

observer at the cost of only a slightly slower transient, but identical steady-state behavior.

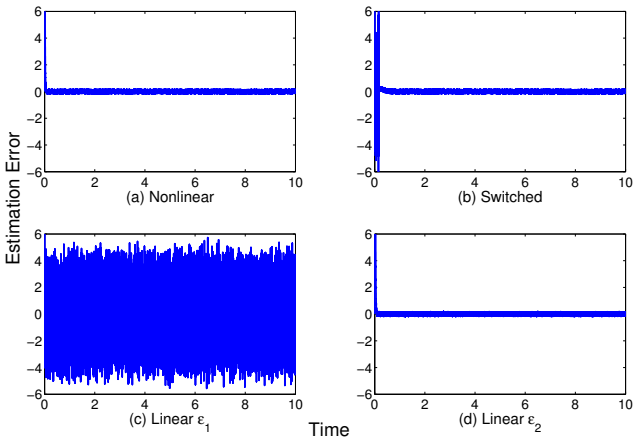

Fig. 3. Steady-state response for the error $x_2 - \hat{x}_2$ vs. time

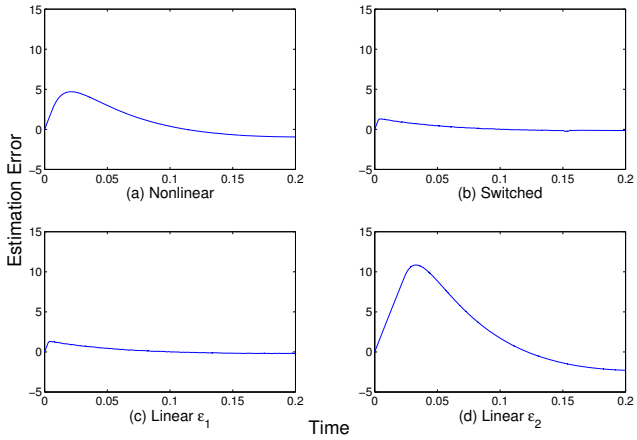

Fig. 4. Transient response for the tracking error $x_2 - \dot{r}$ vs. time

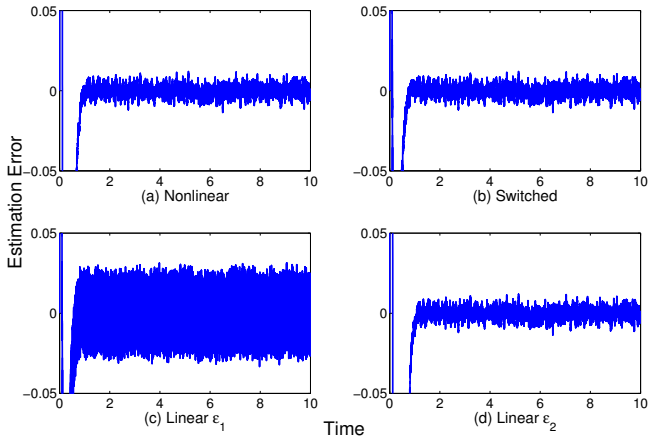

Fig. 5. Steady-state response for the tracking error $x_2 - \dot{r}$ vs. time

V. CONCLUSIONS

This paper investigated a new nonlinear high-gain observer. It was shown that a crucial point in the closed-loop analysis of the fast variables is to design the observer eigenvalues with one eigenvalue much faster than the rest, to ensure that the error $y - \hat{x}_1$ enters the deadzone in finite time. With the nonlinear gain, the trade-off between fast state reconstruction and noise attenuation was predominately minimized. Although this method produces results similar to that of a switched high-gain observer, the nonlinear observer is able to do so without the associated complications due to implementation overhead.

REFERENCES

[1] F. Esfandiari and H. Khalil, "Output feedback stabilization of fully linearizable systems," *Int. J. Contr.*, vol. 56, no. 5, pp. 1007–1037, Nov. 1992.

[2] J. P. Gauthier and I. A. K. Kupka, "Observability and observers for nonlinear systems," *SIAM Journal of Control and Optimization*, vol. 32, no. 4, pp. 975–994, July 1994.

[3] J. P. Gauthier, H. Hammouri, and S. Othman, "A simple observer for nonlinear systems applications to bioreactors," *IEEE Transactions on Automatic Control*, vol. 37, no. 6, pp. 875–880, June 1992.

[4] P. Krishnamurthy and F. Khorrami, "High-gain output-feedback control for nonlinear systems based on multiple time scaling," *Systems and Control Letters*, vol. 56, pp. 7–15, July 2007.

[5] L. Praly and Z. P. Jiang, "Linear output feedback with dynamic high gain for nonlinear systems," *Systems and Control Letters*, vol. 53, pp. 107–116, February 2004.

[6] J. H. Ahrens and H. K. Khalil, "High-gain observers in the presence of measurement noise: A switched-gain approach," *Automatica (Accepted for Publication)*, 2008.

[7] ——, "Output feedback control using high-gain observers in the presence of measurement noise," in *Proc. of the 2004 American Control Conference*, Boston, Massachusetts, June 2004, pp. 4114–4119.

[8] L. K. Vasiljevic and H. K. Khalil, "Differentiation with high-gain observers in the presence of measurement noise," in *Proc. IEEE Conf. on Decision and Control*, San Diego, Califorina, 2006, pp. 4717–4722.

[9] A. Tilli and M. Montanari, "A low-noise estimator of angular speed acceleration from shaft encoder measurements," *Automatika*, vol. 42, pp. 169–176, 2001.

[10] D. Q. Mayne, R. W. Grainger, and G. C. Goodwin, "Nonlinear filters for linear signal models," *Proc. IEEE Control Theory Applications*, vol. 144, pp. 281–286, 1997.

[11] J. H. Ahrens, "Design and performance tradeoffs of high-gain observers with applications to the control of smart material actuated systems," Ph.D. dissertation, Michigan State University, 2006.

[12] L. Fridman, A. Levant, and J. Davila, "High-order sliding mode observer for linear systems with unknown inputs," in *Proceedings of the 2006 International Workshop on Variable Structure Systems*, June 2006, pp. 202–207.

[13] J.-J. E. Slotine, J. K. Hedrick, and E. A. Misawa, "On sliding observer for nonlinear systems," *Journal of Dynamic Systems and Control*, vol. 109, pp. 245–252, 1987.

[14] A. Levant, "Higher-order sliding modes, differentiation and output feedback control," *International Journal of Control*, vol. 76, no. 9, pp. 924–941, September 2003.

[15] S. Spurgeon, "Sliding mode observers: a survey," *International Journal of Systems Science*, vol. 39, no. 8, pp. 751–764, August 2008.

[16] P. Kokotovic, H. K. Khalil, and J. O'Reilly, *Singular Perturbation Methods in Control Analysis and Design*. Philadelphi, PA: SIAM, 1999.

[17] H. K. Khalil, *Nonlinear Systems*, 3rd ed. Upper Saddle River, NJ: Prentice Hall, 2002.